Proceedings of the 28th IEEE
EMBS Annual International Conference
New York City, USA, Aug 30-Sept 3, 2006

Cortical Potential Imaging of Movement-Related Potentials using Parametric Wiener Filter in Realistic-Shaped Head Model

Junichi Hori, *Senior Member*, Bin He, *Fellow, IEEE*

Abstract—**Suitable spatial filters were explored for inverse estimation of cortical potential imaging from the scalp electroencephalogram. The effects of incorporating signal and noise covariance into inverse procedures were examined by computer simulations and experimental study. The parametric Wiener filter (PWF) was applied to an inhomogeneous three-sphere head model under various signal and noise conditions. We also examined estimation methods for the signal covariance in PWF. The present simulation results suggest that the PWF with modified matrix transformation method has better performance. The proposed methods were applied to self-paced movement-related potentials in order to identify the anatomic substrate locations of neural generators in realistic-shaped head model. The proposed methods demonstrated that the contralateral premotor cortex was preponderantly activated in relation to movement performance.**

I. Introduction

ELECTROENCEPHALOGRAPHY (EEG) has been a useful modality to provide high temporal resolution regarding the underlying brain electrical activity. However, the spatial resolution of EEG is limited due to the smearing effect of the head volume conductor. In the past decades, much effort has been made in the development of high-resolution EEG techniques, which attempt to map spatially distributed brain electrical activity with substantially improved spatial resolution without *ad hoc* assumption on the number of source dipoles. Of particular interest is the recent development of cortical imaging approaches, in which an explicit biophysical model of the passive conducting properties of a head is used to deconvolve a measured scalp potential distribution into a distribution of electrical potential on the cortical surface [1]-[11]. Because the cortical-potential distribution can be experimentally measured [4], [12] and compared to the inverse imaging results, the cortical potential imaging approach is also of physiologic importance.

In parallel to the development of physical models for cortical potential imaging, the regularization algorithm plays an important role in ill-posed cortical inverse problem. Regularization strategies, such as general inverse with truncated singular value decomposition (SVD), constrained least square method, and Tikhonov regularization method, have been used to solve the ill-conditioned cortical imaging inverse problem (for review, see [1]). We have previously developed the parametric projection filter (PPF) based cortical dipole layer imaging technique, which allows estimating cortical dipole layer inverse solutions in the presence of noise covariance [13]-[15]. Our previous results indicate that the results of the PPF provide better approximation to the original dipole layer distribution than that of traditional inverse techniques in the case of low correlation between signal and noise distributions. Moreover, we have tested the proposed method in effectively rejecting time-variant noise such as eyes blink artifact [15]. Wiener reconstruction frameworks based on both signal and noise covariance matrices have been also investigated [3], [16]-[19]. We have studied the restorative abilities of the parametric Wiener filter (PWF) as compared with the PPF in simulation of cortical dipole layer imaging [20].

In the present study, the performance of the proposed PWF for cortical potential imaging has been evaluated by computer simulation under various noise conditions for inhomogeneous volume conductor head model [8]. We have also improved the algorithm to estimate the signal covariance in PWF.

Moreover, the proposed method is applied for movement-related potentials (MRP) of fast repetitive finger movement protocols [21]-[24]. We utilize cortical potential imaging projected onto the realistic-shaped cortical surface to locate the possible generators of MRPs in human.

II. Method

A. Principles of Cortical Potential Imaging

In the present cortical potential imaging study, the head volume conductor is approximated by the inhomogeneous three-concentric sphere model and a closed dipole layer of 1280 dipoles are used [8]. This head model takes the variation in conductivity of different tissues, such as the scalp, the skull and the brain, into consideration.

The observation system of brain electrical activity on the scalp shall be defined by

$$g = A f + n \qquad (1)$$

where f is the vector of the equivalent source distribution of a dipole layer, n is the vector of the additive noise and g is the vector of scalp-recorded potentials. A represents the transfer matrix from the equivalent source to the scalp potentials. The

Manuscript received April 3, 2006. This work was supported in part by a Grant for Promotion of Niigata University Research Projects, JSPS Grants-in-Aid for Scientific Research 17500349, NIH R01EB00178, and NSF BES-0411898.

J. Hori is with the Department of Biocybernetics, Niigata University, Niigata 950-2181 Japan (phone: 81-25-262-6733; fax: 81-25-262-7010; e-mail: hori@bc.niigata-u.ac.jp).

B. He is with Department of Biomedical Engineering, University of Minnesota, Minneapolis, 55455 USA (e-mail: binhe@umn.edu).

estimated source distribution of the dipole layer f_0 shall be defined by

$$f_0 = B\, g \qquad (2)$$

where B is the restoration filter. Once f_0 is estimated, the potential distribution on the cortical surface can be calculated through forward solution using the transfer matrix from the equivalent dipole layer to the cortical potentials [8]. In the case of spatiotemporal inverse problem, this procedure would be applied to every time constant.

B. Inverse Techniques

When the statistical information of signal and noise are presented, the Wiener filter can be applied to the inverse problem [3], [8]. Suppose R and Q the signal and the noise covariance, which can be derived from the expectation over the signal $\{f\}$ and noise $\{n\}$ ensemble, $E[f f^*]$ and $E[n\, n^*]$, respectively. f^* and n^* are the transpose of f and n, respectively. The PWF is derived by

$$B = R A^* (A\, R\, A^* + \gamma Q)^{-1}. \qquad (3)$$

with γ a small positive number known as the regularization parameter. Since the signal and noise are time-variant in EEG measurements, the signal and noise covariance, and the regularization parameter were supposed to be time-variant. If $R = Q = I$ (the identity matrix), then equation (3) is reduced to the zero-order Tikhonov regularization method. The PWF has been applied to brain source imaging [16], [17]. The PPF considers just the covariance matrix of the noise distribution Q that is, $R = I$ in (3) [13]-[15]. The restoration filter (3) has a free parameter γ that determines the restorative ability. We have developed a new criterion that estimates the optimum parameter using iterative calculation for restoration [13]. The criterion estimates the parameter that minimizes the approximated error between the original and estimated source signals without knowing the original source distribution. In a clinical and experimental setting, the noise covariance Q may be estimated from data that is known to be source free. The signal covariance, R, is calculated using observed scalp potentials, the transfer function, and estimated noise covariance [16],[19]. We compared three estimation methods for the signal covariance:

1) SVD method [16]

The covariance of the observed signals P is calculated by

$$P = E[g\, g^*] \qquad (4)$$

and has a SVD given by $P = U \Lambda U^*$ where U is the eigenvectors and Λ is the diagonal composed with eigenvalues. A measure for i-th source signal is defined by

$$\xi_i = A_i^* U \Lambda^{-1} U^* A_i / (A_i^* A_i). \qquad (5)$$

The diagonal of the signal covariance matrix weighted by (5) can be estimated by $R_{ii} = f(1 / \xi_i)$ where f is a continuous, nondecreasing function.

2) Matrix transformation [19]

Substituting (1) into (4), we can obtain

$$P = A\, R\, A^* + Q. \qquad (6)$$

The signal covariance R can be obtained by

$$R = A^{-1} (P - Q) (A^{-1})^* \qquad (7)$$

where A^{-1} is the Moore-Penrose generalized inverse of A.

3) Modified matrix transformation

Moore-Penrose generalized inverse A^{-1} in (7) can be calculated by the zero-order Tikhonov regularization. From the results of previous simulations, the PWF provided better performance than the Tikhonov regularization in restoration [13], [14]. Thus, R can be calculated using the PWF, B, in (3) instead of A^{-1} provided that the initial inverse filter B is constructed with (3) using R in (7).

C. Simulation

We have applied PWF to the inverse problem of the cortical potential imaging in inhomogeneous spherical head model. Two radial dipoles, located at the center position were used as the sources. The restorative abilities of above three estimation methods were compared under various noise configurations such as uniform Gaussian white noise (GWN) and edge-, center-, and one side-concentrated non-uniform noise. Suitable dipole layer setting was also examined in various signal configurations.

D. Human Experimentation

A right-handed female normal subject with age of 24 years took part in the present study after informed consent was obtained according to the Institutional Review Board. The subject performed fast repetitive finger movements which were cued by visual stimuli. 10-15 blocks of 2 Hz thumb oppositions for both hands were recorded, with each 30 second blocks of finger movement and rest.

Using a 96-channel EEG system (NeuroScan Lab, TX), electrical potentials were recorded from 94 scalp sensors. A/D sampling rate was 250 Hz. One bipolar EMG was recorded and the peak point of EMG was used as a trigger for the MRP averaging. All data were visually inspected, and trials containing artifacts were rejected. After the EEG recording, the electrode positions were digitized using a 3D localization device with respect to the anatomic landmarks of the head (nasion and two preauricular points). EMG-locked averaging was done off-line. About 450 artifact-free single epochs were averaged according to the following procedure. The EEG data were digitally filtered with a band-pass of 0.3-50 Hz. The noise covariance of the PWF was estimated by the EEG data at the time point of EMG peak. The signal covariance was estimated by non-averaged EEG data at the period of motor field (MF). The estimated cortical potential distributions are projected onto the realistic-shaped cortical surface.

III. Results

Fig. 1 shows the relative error (RE) between actual and estimated cortical potentials against the noise level (NL) in

three inverse techniques. The eccentricity of the dipole sources is 0.7 and the angle of two radial dipoles is 30 degrees. The radius of dipole layer is set to 0.8. Modified matrix translation method has better performance than others for every noise configurations. On the other hand, the RE of SVD method changed slightly whenever the NL became large.

Equivalent dipole layer can be placed at arbitrary depth between cortical surface and sources. However, the results will be improved by considering the signal and noise conditions and setting optimum depth for dipole layer. We examined the RE between actual and estimated cortical potentials against the radius of dipole layer in the case of 5% GWN (Fig. 2). The dipole layer was set at the outside of the sources. When the sources were deep-seated, the RE became large. Moreover, the RE became the minimum when the eccentricity of the dipole layer was about 0.8.

Cortical dipole imaging analysis of the MRPs was conducted during the period of the MF. For dipole imaging, the time point with the highest activity in the period of MF waveform was determined to be around 50 ms after the peak of EMG. Fig. 3 displays the estimated results of the cortical potential imaging for right hand movement and left hand movement. Note that the cortical potential distributions estimated by means of PWF based on modified matrix transformation were well-localized as compared with blurred scalp potential maps. As shown in realistic-shaped cortical surface, the localized areas for MF in both hands were located in the premotor cortex, which is consistent with the hand motor representation. Most activities of the source in right-hand movement in the period of the MF covered the precentral sulcus. Fig. 3 also indicates that the location of right hand movement activity seems more temporal than the activity in left hand movement. These results were coincide with [23].

IV. Discussion

We have initially investigated the performance of cortical potential imaging by considering signal and noise covariance through the use of PWF. The noise covariance may be estimated from data that is known to be source free, such as prestimulus data in evoked potentials in a clinical situation. In MRPs, prominent features including a pre- and post-movement peak have been reported [21], [22]. Thus, we calculated the noise covariance at the time point of EMG peak that is between pre and post movement. The SVD-based method [16] and matrix transformation method [19] were proposed previously for signal covariance estimation. The SVD method was robust for noise because signal and noise space are gradually distinguished by weight factors based on eigenvalues. On the other hand, the matrix transformation method can be easily derived from matrix operations. By replacing the Moore-Penrose generalized inverse with the PWF, we could obtain improved results. This procedure can be applied to the inverse problem iteratively.

Theoretically, even if the radius of a dipole layer changes the estimated cortical potentials is considered to be identical each other. However, in actual situation, the signals are contaminated with noise and the forward and inverse procedures produce calculation error. From the simulation results, the relative error became the minimum when the dipole layer was set at the middle point between cortical surface and sources. When the sources and the dipole layer are near, the equivalent dipole source distribution becomes sharp and it is hard to estimate precisely. Moreover, when the sources and the dipole layer are far, it is considered that the rounding error in calculation is contained in the transfer function from a dipole layer to the brain surface. Therefore, if we know a priori information on the location of the sources by anatomical constraint, the ideal position of a dipole layer may be determined.

Cortical potential imaging can provide the electrical potential on cortical surface while cortical dipole layer imaging represents the electrical activity distribution in side of the brain by spherical shaped equivalent dipole layer. In human experimental study, cortical potential imaging is suitable for representing the distributions of the results by projection onto the realistic shaped cortical surface. The present experimental study indicates that contralateral predominant activity of MF would occur after the EMG peak for both hands, which extends previous evidence supporting a hemispheric functional asymmetry of motor control.

The authors thank Takeshi Ohshima and Toshinari Miwa for their experimental help.

References

[1] B. He, “Brain Electric Source Imaging – Scalp Laplacian mapping and cortical imaging,” *Crit. Rev. BME*, vol. 27:149-188, 1999.

[2] R. Sidman, M. Ford, G. Ramsey, and C. Schlichting, “Age-related features of the resting and P300 auditory evoked responses using the dipole localization method and cortical imaging technique,” *J. Neurosci. Meth.,* vol. 33, pp. 23-32, 1990.

[3] R. Srebro, R. M. Oguz, K. Hughlett, and P. D. Purdy, “Estimating regional brain activity from evoked potential field on the scalp,” *IEEE Trans. Biomed. Eng.*, vol. 40, pp. 509-516, 1993.

[4] A. Gevins, J. Le, N. K. Martin, P. Brickett, J. Desmond, and B. Reutter, “High resolution EEG: 124-channel recording, spatial deblurring and MRI integration methods,” *Electroenceph. Clin. Neurophysiol.*, vol. 90, pp. 337-358, 1994.

[5] P. Nunez, R. B. Silibertein, P. J. Cdush, R. S. Wijesinghe, A. F. Westdrop, and R. Srinivasan, “A theoretical and experimental study of high resolution EEG based on surface Laplacian and cortical imaging,” *Electroenceph. Clin. Neurophysiol.*, vol. 90, pp. 40-57, 1994.

[6] B. He, Y. Yang, S. Pak, and Y. Ling, “Cortical source imaging from scalp electroencephalograms,” *Med. Biol. Eng. Comput.*, vol. 34, suppl., pt. 2, pp. 257-258, 1996.

[7] F. Babiloni, C. Babiloni, F. Carducci, L. Fattorini, C. Anello, P. Onorati, and A. Urbano, “High resolution EEG: a new model-dependent spatial deblurring method using a realistically-shaped MR-constructed subject's head model,” *Electroenceph. Clin. Neurophysiol.*, vol. 102, pp. 69-80, 1997.

[8] Y. Wang and B. He, “A computer simulation study of cortical imaging from scalp potentials,” *IEEE Trans. Biomed. Eng.*, vol. 45, pp. 724-735, 1998.

[9] G. Edlinger, P. Wach, and G. Pfurtscheller, “On the realization of an analytic high-resolution EEG,” *IEEE Trans. Biomed. Eng.*, vol. 45, pp. 736-745, 1998.

[10] B. He, Y. Wang, and D. Wu, "Estimating cortical potentials from scalp EEG's in a realistically shaped inhomogeneous head model," *IEEE Trans. Biomed. Eng.*, vol. 46, pp. 1264-1268, 1999.
[11] B. He, J. Lian, K. M. Spencer, J. Dien, and E. Donchin, "A cortical potential imaging analysis of the P300 and novelty P3 components," *Human Brain Mapping*, vol. 12: pp. 120-130, 2001.
[12] V. L. Towle, S. Cohen, N. Alperin, K. Hoffmann, P. Cogsen, J. Milton, R. Grzeszczuk, C. Pelizzari, I. Syed, and J. P. Spire, "Displaying electrocorticographic findings on gyral anatomy," *Electroenceph. clin. Neurophysiol,* vol. 94, pp. 221-228, 1995.
[13] J. Hori and B. He, "Equivalent dipole source imaging of brain electric activity by means of parametric projection filter," *Annals Biomed. Eng.*, vol. 29, pp. 436-445, 2001.
[14] J. Hori and B. He, "EEG Cortical potential imaging of brain electrical activity by means of parametric projection filters," *IEICE Trans. Inf. & Syst.*, vol.E86-D, no.9, pp.1909-1920, Sep. 2003.
[15] J. Hori, M. Aiba, and B. He, "Spatio-temporal dipole source imaging of brain electrical activity by means of time-varying parametric projection filter," *IEEE Trans. Biomed. Eng.*, vol.51, no.5, pp.768-777, May 2004.
[16] A. M. Dale and M. I. Sereno, "Improved localization of cortical activity by combining EEG and MEG with MRI cortical surface reconstruction: a linear approach," *J. Cognitive Neuroscience*, vol. 5, pp. 162-176, 1993.
[17] J. W. Philips, R. M. Leahy, and J. C. Mosher, "MEG-based imaging of focal neuronal current sources," *IEEE Trans. Med. Imaging*, vol. 16, pp. 338-348, 1997.

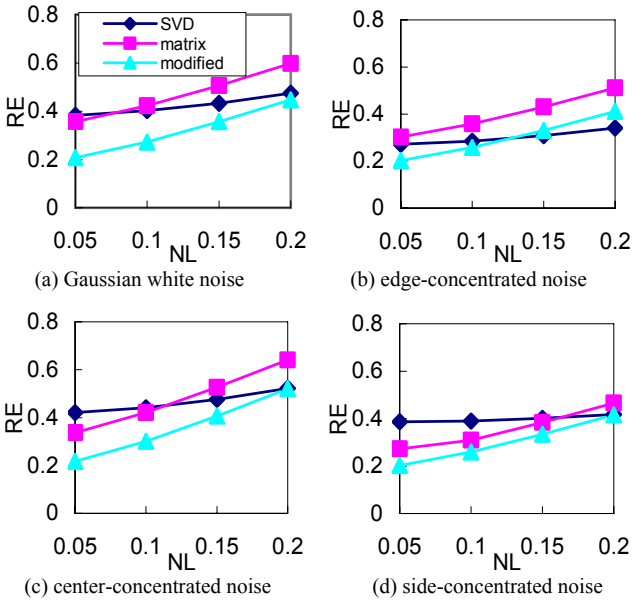

(a) Gaussian white noise (b) edge-concentrated noise

(c) center-concentrated noise (d) side-concentrated noise

Fig. 1. Simulation results of relative error between actual and estimated cortical maps against the noise level in three estimation methods. The eccentricity of dipole sources is 0.7.

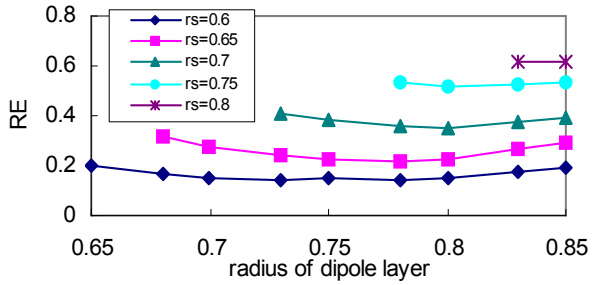

Fig. 2. Simulation results of relative Error between actual and estimated cortical maps against the radius of dipole layer. The eccentricity of dipole sources r_s is 0.6-0.8.

[18] R. Grave de Peralta Menendez and S. L. Gonzalez Andino, "Distributed source models: standard solutions and new developments," In: Uhl, C. (ed): *Analysis of neurophysiological brain functioning*, Springer Verlag, pp. 176-201, 1998.
[19] K. Sekihara and B. Scholz, "Average-intensity reconstruction and Wiener reconstruction of bioelectric current distribution based on its estimated covariance matrix," *IEEE Trans. Biomed. Eng.*, vol. 42, pp. 149-157, 1995.
[20] J. Hori, T. Miwa, T. Ohshima, and B. He, "Cortical dipole imaging of movement-related potentials by means of parametric inverse filters incorporating with signal and noise covariance", *Methods Inf. Med.*, (in press).
[21] C. Gerloff, C. Toro, N. Uenishi, L.G. Cohen, L. Leocani, and M. Hallett, "Steady-state movement-related cortical potentials: a new approach to assessing cortical activity associated with fast repetitive finger movements," *Electroencephal. Clin. Neurophysiol.*, vol. 102, pp. 106-113, 1997.
[22] C. Gerloff, N. Uenishi, T. Nagamine, T. Kunieda, M. Hallett, and H. Shibasaki, "Cortical activation during fast repetitive finger movements in humans: steady-state movement-related magnetic fields and their cortical generators," *Electroenceph. Clin. Neurophysiol.*, vol. 109, pp. 444-453, 1998.
[23] Y. Ni, L. Ding, J. Cheng, K. Christine, J. Lian, X. Zhang, N. Grusazuskas, J. Sweeney, and B. He, "EEG source analysis of motor potentials induced by fast repetitive unilateral finger movement," *Proc. 1st IEEE-EMBS Int. Conf. Neural Eng.*, Mar. 2003.
[24] F. Babiloni, C. Babiloni, F. Carducci, F. Cincotti, L. Astolfi, A. Basilisco, P.M. Rossini, L. Ding, Y. Ni, J. Cheng, K. Christine, J. Sweeney, and B. He, "Assessing time-varying cortical functional connectivity with the multimodal integration of high resolution EEG and fMRI data by directed transfer function," *NeuroImage*, vol. 24, pp. 118-131, 2005.

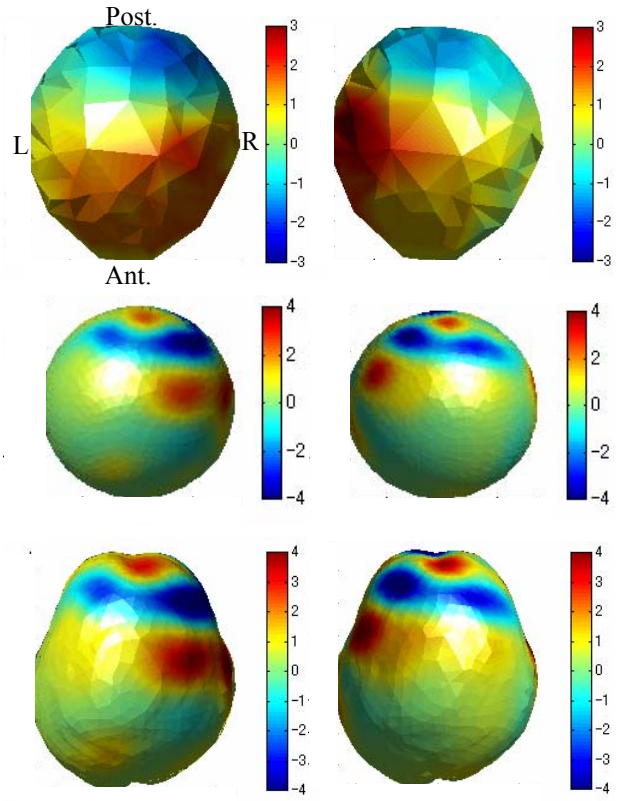

Fig. 3. Scalp potential maps (top) measured in the period of the motor field for right hand movement (left) and left hand movement (right), respectively. Cortical potential images estimated by PWF in spherical model (middle) and realistic-shaped model (bottom).